

# Low-complexity Linear Equalization for OTFS Modulation

G. D. Surabhi and A. Chockalingam

**Abstract**—In this letter, we propose low-complexity linear equalizers for orthogonal time frequency space (OTFS) modulation that exploit the structure of the effective channel matrix in OTFS. The proposed approach exploits the block circulant nature of the OTFS channel matrix to achieve significant complexity reduction. For an  $N \times M$  OTFS system, where  $N$  and  $M$  are the number of Doppler and delay bins, respectively, the proposed approach gives exact minimum mean square error (MMSE) and zero-forcing (ZF) solutions with just  $\mathcal{O}(MN \log MN)$  complexity, while MMSE and ZF solutions using the traditional matrix inversion approach require  $\mathcal{O}(M^3N^3)$  complexity. The proposed approach can provide low complexity initial solutions for local search techniques to achieve enhanced bit error performance.

**Keywords:** OTFS modulation, linear equalizers, block circulant matrices, computational complexity.

## I. INTRODUCTION

The challenge of establishing reliable high-speed communication in extremely dynamic environments has been addressed recently by a new modulation technique called the ‘orthogonal time frequency space (OTFS)’ modulation. It has been shown that the OTFS modulation achieves superior bit error rate performance (BER) compared to the conventional multicarrier techniques like orthogonal frequency division multiplexing (OFDM), in very high Doppler wireless environments. The fundamental premise of OTFS modulation is the representation of the channel and the information symbols in the delay-Doppler domain rather than the time-frequency domain as done in conventional multicarrier modulation techniques. A key advantage of the delay-Doppler representation of wireless channels is that the rapid fluctuation of the time varying channel exhibits slow variations when viewed in the delay-Doppler domain. This, along with the fact that the channel in the delay-Doppler domain has a sparse nature, simplifies channel estimation in rapidly time varying wireless channels.

OTFS modulation was first proposed in [1], where it was demonstrated to have superior error performance compared to OFDM in very high Doppler environments. This was followed by several works addressing various aspects of OTFS modulation [2]-[8]. Low complexity detection of OTFS signal has been addressed using message passing based detector and Markov chain Monte Carlo based algorithm in [3] and [4], respectively. Further, while [6] uses a minimum mean squared error (MMSE) detector for OTFS signal detection, [7] proposes an interference cancellation based low-complexity

equalizer followed by an initial MMSE equalization in time-frequency domain. The performance of OTFS modulation with MMSE equalizer and decision feedback equalizer has been discussed in [2]. It has been shown in [2] that the BER performance of uncoded OTFS with MMSE equalizer is significantly better compared to that of OFDM for lower modulation order (BPSK, 4-QAM, and 16-QAM) and the performance gains degrade for higher order QAM (64-QAM and 256-QAM). It has also been suggested in [2] that this performance can be improved significantly by the use of a non-linear equalizer following a linear equalizer. Motivated by this and the fact that the overall detection complexity can reduce by reducing the complexity of the linear equalizer preceding the non-linear equalizer, in this letter, we propose low-complexity linear equalizers for OTFS signal detection. Our novel approach in this effort is the exploitation of the structure prevalent in the effective channel matrix in OTFS to reduce the computational complexity of linear equalizers, which has not been reported before.

We propose low-complexity MMSE and zero-forcing (ZF) equalizers for OTFS signal detection, which do not rely on the traditional matrix inversion approach that conventional MMSE and ZF equalizers employ. Instead, the proposed approach achieves exact MMSE and ZF solutions at a much lower complexity compared to the matrix inversion approach. This is made possible by recognizing a certain structure in the effective delay-Doppler channel matrix in OTFS modulation. Specifically, the proposed approach recognizes the block circulant nature of the OTFS channel matrix and exploits the properties of block circulant matrices to achieve significant complexity reduction. For example, for an  $N \times M$  OTFS system, where  $N$  and  $M$  are the number of Doppler and delay bins, respectively, the complexity of MMSE and ZF equalizers using the conventional matrix inversion approach is  $\mathcal{O}(M^3N^3)$ , whereas the proposed approach gives exact MMSE and ZF solutions using a computation complexity of just  $\mathcal{O}(MN \log MN)$ . This complexity reduction of linear equalizers can aid efficient realizations of non-linear equalizers to achieve enhanced bit error performance at reduced overall complexity. We illustrate this by using the proposed MMSE equalizer solution as the initial solution to a local search based non-linear equalizer.

## II. OTFS MODULATION

We consider OTFS modulation architected over a general multicarrier modulation system as shown in Fig. 1. The transforms involved in OTFS modulation and demodulation are introduced in the following subsections.

### A. OTFS transmitter

The OTFS transmitter considers  $NM$  information symbols on an  $N \times M$  delay-Doppler grid, denoted by  $x[k, l]$ ,  $k = 0, \dots, N - 1$ ,  $l = 0, \dots, M - 1$  from a modulation alphabet  $\mathbb{A}$ , to be transmitted in a given packet burst of duration  $NT$ , occupying a bandwidth of  $B = M\Delta f$ , where

Copyright (c) 2019 IEEE. Personal use of this material is permitted. However, permission to use this material for any other purposes must be obtained from the IEEE by sending a request to pubs-permissions@ieee.org.

Manuscript received October 18, 2019; revised November 22; accepted November 22, 2019. The editor coordinating the review of this manuscript and approving it for publication was Prof. Fanggang Wang.

This work was supported in part by the J. C. Bose National Fellowship, Department of Science and Technology, Government of India, Tata Elxsi Limited, Bengaluru 560048, and the Intel India Faculty Excellence Program. The authors are with the Department of Electrical Communication Engineering, Indian Institute of Science, Bengaluru 560012, India (e-mail: surabhi@iisc.ac.in; achockal@iisc.ac.in).

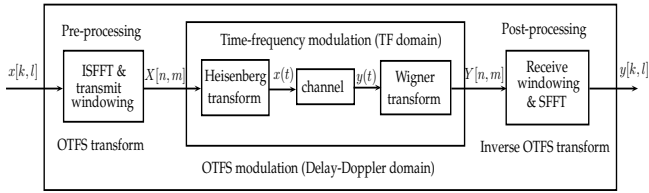


Fig. 1: OTFS modulation scheme.

$\Delta f = 1/T$ . The information symbols  $x[k, l]$ s are treated as points on the 2D  $N \times M$  delay-Doppler grid and are mapped to time-frequency plane using inverse symplectic finite Fourier transform (ISFFT), given by

$$X[n, m] = \frac{1}{MN} \sum_{k=0}^{N-1} \sum_{l=0}^{M-1} x[k, l] e^{j2\pi(\frac{nk}{N} - \frac{ml}{M})}. \quad (1)$$

The TF signal so obtained is converted to time domain for transmission using Heisenberg transform, given by

$$x(t) = \sum_{n=0}^{N-1} \sum_{m=0}^{M-1} X[n, m] g_{tx}(t - nT) e^{j2\pi m \Delta f (t - nT)}, \quad (2)$$

where  $g_{tx}(t)$  denotes the transmit pulse shape. The time domain signal  $x(t)$  is then transmitted through the time varying wireless channel. Denoting the complex baseband response of the channel in delay-Doppler domain by  $h(\tau, \nu)$ , where  $\tau$  and  $\nu$  are delay and Doppler variables, respectively, the received time domain signal is given by

$$y(t) = \int_{\nu} \int_{\tau} h(\tau, \nu) x(t - \tau) e^{j2\pi\nu(t - \tau)} d\tau d\nu. \quad (3)$$

### B. OTFS receiver

At the receiver, the received time domain signal  $y(t)$  is transformed into a TF signal using Wigner transform, which match filters  $y(t)$  with received pulse shape  $g_{rx}(t)$  and samples it at the lattice points  $t = nT$  and  $f = m\Delta f$ . The Wigner transform is given by

$$A_{g_{rx}, y}(t, f) = \int g_{rx}^*(t' - t) y(t') e^{-j2\pi f(t' - t)} dt',$$

$$Y[n, m] = A_{g_{rx}, y}(t, f)|_{t=nT, f=m\Delta f}. \quad (4)$$

If the transmit pulse  $g_{tx}(t)$  and the receive pulse  $g_{rx}(t)$  satisfy biorthogonality and robustness condition in [2], the input-output relation of the TF modulation is given by

$$Y[n, m] = H[n, m]X[n, m] + V[n, m], \quad (5)$$

where  $V[n, m]$  is the additive white Gaussian noise (AWGN) at the output of Wigner transform, and  $H[n, m]$  is given by

$$H[n, m] = \int_{\tau} \int_{\nu} h(\tau, \nu) e^{j2\pi\nu nT} e^{-j2\pi(\nu + m\Delta f)\tau} d\nu d\tau. \quad (6)$$

The TF signal  $Y[n, m]$  so obtained is mapped back to the delay-Doppler domain using symplectic finite Fourier transform (SFFT), given by

$$y[k, l] = \sum_{n=0}^{N-1} \sum_{m=0}^{M-1} Y[n, m] e^{-j2\pi(\frac{nk}{N} - \frac{ml}{M})}. \quad (7)$$

Using (1)-(7), the input-output relation can be derived as [2]

$$y[k, l] = \frac{1}{MN} \sum_{l'=0}^{M-1} \sum_{k'=0}^{N-1} x[k', l'] h_w\left(\frac{k-k'}{NT}, \frac{l-l'}{M\Delta f}\right) + v[k, l], \quad (8)$$

where  $h_w\left(\frac{k-k'}{NT}, \frac{l-l'}{M\Delta f}\right) = h_w(\nu, \tau)|_{\nu=\frac{k-k'}{NT}, \tau=\frac{l-l'}{M\Delta f}}$  and  $h_w(\nu, \tau)$  is the circular convolution of the channel response with a windowing function  $w(\nu, \tau)$  as defined in [2]. The above equation can be vectorized as [3]

$$\mathbf{y} = \mathbf{H}\mathbf{x} + \mathbf{n}, \quad (9)$$

where  $\mathbf{x} \in \mathbb{C}^{MN \times 1}$ ,  $\mathbf{x}_{k+NI} = x[k, l] \in \mathbb{A}$ ,  $\mathbf{y} \in \mathbb{C}^{MN \times 1}$  is the received vector,  $\mathbf{H} \in \mathbb{C}^{MN \times MN}$  is the effective channel matrix in delay-Doppler domain, and  $\mathbf{n} \in \mathbb{C}^{MN \times 1}$  is the AWGN vector whose entries are distributed as  $\mathcal{CN}(0, \sigma^2)$ .

### III. LOW-COMPLEXITY LINEAR RECEIVERS FOR OTFS

Consider the vectorized input-output relation in OTFS given by (9). The estimates of the transmitted symbols at the output of a linear receiver will be of the form  $\hat{\mathbf{x}} = f(\mathbf{G}\mathbf{y})$ , where  $\mathbf{G}$  is a linear transformation matrix which depends on the type of linear receiver and  $f(\cdot)$  is a function that maps each entry of the vector  $\mathbf{G}\mathbf{y}$  to the nearest symbol in the modulation alphabet  $\mathbb{A}$  in terms of Euclidean distance. The linear transformation matrices for MMSE and ZF are given by  $\mathbf{G}_{\text{MMSE}} = (\mathbf{H}^H \mathbf{H} + \sigma^2 \mathbf{I})^{-1} \mathbf{H}^H$  and  $\mathbf{G}_{\text{ZF}} = (\mathbf{H}^H \mathbf{H})^{-1} \mathbf{H}^H$ , respectively. Observe that the computation of both  $\mathbf{G}_{\text{MMSE}}$  and  $\mathbf{G}_{\text{ZF}}$  involves inversion of  $MN \times MN$  matrices, which has a computational complexity of  $\mathcal{O}(M^3 N^3)$ . This is not attractive for large values of  $M$  and  $N$ . The computation of  $\mathbf{G}_{\text{MMSE}}$  and  $\mathbf{G}_{\text{ZF}}$  can be achieved with significantly lower complexity if the structures of  $\mathbf{H}$ ,  $\mathbf{G}_{\text{MMSE}}$ , and  $\mathbf{G}_{\text{ZF}}$  are carefully exploited.

#### A. Low-complexity MMSE equalizer

Consider the vectorized input-output relation in (9). The  $MN \times MN$  channel matrix  $\mathbf{H}$  in (9) is a block circulant matrix with  $M$  circulant blocks, each of size  $N \times N$ . Let  $\mathcal{B}_{M,N}$  denote the class of block circulant matrices with  $M$  circulant blocks of size  $N \times N$ . Denoting circulant matrices with  $\text{circ}(\cdot)$ , any matrix  $\mathbf{A} \in \mathcal{B}_{M,N}$  will be of the form  $\text{circ}(\mathbf{A}_0, \mathbf{A}_1, \dots, \mathbf{A}_{M-1})$ , where each block  $\mathbf{A}_i$  is an  $N \times N$  circulant matrix of the form  $\text{circ}(a_{i,0}, a_{i,1}, \dots, a_{i,N-1})$  [11].

In order to derive the low-complexity MMSE detector for OTFS, we make use of the following three properties of  $\mathcal{B}_{M,N}$ .

- 1) Any matrix  $\mathbf{A} \in \mathcal{B}_{M,N}$  is diagonalized by the unitary matrix  $(\mathbf{F}_M \otimes \mathbf{F}_N)$ , where  $\mathbf{F}_M$  and  $\mathbf{F}_N$  denote discrete Fourier transform (DFT) matrices of size  $M \times M$  and  $N \times N$ , respectively, and  $\otimes$  denotes the Kronecker product of two matrices [11]. Hence,  $\mathbf{A}$  can be written as

$$\mathbf{A} = (\mathbf{F}_M \otimes \mathbf{F}_N)^H \mathbf{D} (\mathbf{F}_M \otimes \mathbf{F}_N), \quad (10)$$

where  $\mathbf{D} = \text{diag}\{d_1, d_2, \dots, d_{MN}\}$  and  $d_i$  denotes the  $i$ th eigen value of  $\mathbf{A}$ .

- 2) For any matrix  $\mathbf{A} \in \mathcal{B}_{M,N}$ , the entries of the matrix  $\mathbf{D}$  will be of the form

$$\mathbf{D} = \sum_{i=0}^{M-1} \Omega_M^i \otimes \mathbf{D}_i, \quad (11)$$

where  $\Omega_M = \text{diag}\{1, \omega, \dots, \omega^{M-1}\}$  with  $\omega = e^{j2\pi/M}$  and  $\mathbf{D}_i$  denotes the  $N \times N$  diagonal matrix containing the eigen values of the  $N \times N$  circulant block  $\mathbf{A}_i$ .

- 3) For any two matrices  $\mathbf{A}, \mathbf{B} \in \mathcal{B}_{M,N}$ , the matrices  $\mathbf{A}^T$ ,  $\mathbf{A}^H$ ,  $\mathbf{A}\mathbf{B}$  ( $=\mathbf{B}\mathbf{A}$ ),  $\gamma_1 \mathbf{A} + \gamma_2 \mathbf{B}$ ,  $\sum_{r=0}^{R-1} \gamma_r \mathbf{A}^r$ , and  $\mathbf{A}^{-1}$  (if it exists) are all in  $\mathcal{B}_{M,N}$ , where  $\gamma_0, \dots, \gamma_{R-1}$  are scalars.

Now, consider the OTFS channel matrix in (9), which is a block circulant matrix with  $M$  blocks each of size  $N \times N$ . Since  $\mathbf{H} \in \mathcal{B}_{M,N}$ , it can be decomposed as

$$\mathbf{H} = (\mathbf{F}_M \otimes \mathbf{F}_N)^H \mathbf{\Lambda} (\mathbf{F}_M \otimes \mathbf{F}_N), \quad (12)$$

where  $\mathbf{\Lambda} = \text{diag}\{\lambda_1, \lambda_2, \dots, \lambda_{MN}\}$  and  $\lambda_i$  denotes the  $i$ th eigen value of  $\mathbf{H}$ . Next, consider the transformation matrix  $\mathbf{G}_{\text{MMSE}} = (\mathbf{H}^H \mathbf{H} + \sigma^2 \mathbf{I})^{-1} \mathbf{H}^H$ . From property 3), it can be seen that if  $\mathbf{H} \in \mathcal{B}_{M,N}$ , then  $\mathbf{G}_{\text{MMSE}} \in \mathcal{B}_{M,N}$ . Therefore, the eigen value decomposition of  $\mathbf{G}_{\text{MMSE}}$  will be of the form

$$\mathbf{G}_{\text{MMSE}} = (\mathbf{F}_M \otimes \mathbf{F}_N)^H \mathbf{\Psi} (\mathbf{F}_M \otimes \mathbf{F}_N), \quad (13)$$

where  $\mathbf{\Psi}$  is a diagonal matrix of size  $MN \times MN$  containing the eigen values of  $\mathbf{G}_{\text{MMSE}}$ . Substituting (12) in  $\mathbf{G}_{\text{MMSE}} = (\mathbf{H}^H \mathbf{H} + \sigma^2 \mathbf{I})^{-1} \mathbf{H}^H$  and simplifying, we get

$$\mathbf{G}_{\text{MMSE}} = (\mathbf{F}_M \otimes \mathbf{F}_N)^H (\mathbf{\Lambda}^* \mathbf{\Lambda} + \sigma^2 \mathbf{I})^{-1} \mathbf{\Lambda}^* (\mathbf{F}_M \otimes \mathbf{F}_N). \quad (14)$$

Now, comparing (13) and (14),  $\mathbf{\Psi}$  can be written as

$$\mathbf{\Psi} = (\mathbf{\Lambda}^* \mathbf{\Lambda} + \sigma^2 \mathbf{I})^{-1} \mathbf{\Lambda}^*. \quad (15)$$

Therefore, the eigen values of  $\mathbf{G}_{\text{MMSE}}$  can be expressed in terms of the eigen values of  $\mathbf{H}$  as

$$\mathbf{\Psi} = \text{diag} \left\{ \frac{\lambda_1^*}{|\lambda_1|^2 + \sigma^2}, \frac{\lambda_2^*}{|\lambda_2|^2 + \sigma^2}, \dots, \frac{\lambda_{MN}^*}{|\lambda_{MN}|^2 + \sigma^2} \right\}. \quad (16)$$

From (16), it is clear that the eigen values of  $\mathbf{G}_{\text{MMSE}}$  can be computed from the eigen values of  $\mathbf{H}$ . The computation of eigen values of  $\mathbf{G}_{\text{MMSE}}$  using the eigen values of  $\mathbf{H}$  is one of the key steps in the proposed low-complexity MMSE equalizer for OTFS. Using  $\mathbf{G}_{\text{MMSE}}$ , the transmitted symbols are estimated by computing  $\mathbf{G}_{\text{MMSE}} \mathbf{y}$  with significantly lower complexity using FFTs, IFFTs, and the properties of  $\mathbf{H}$  and  $\mathbf{G}_{\text{MMSE}}$  as follows.

- 1) *Computation of eigen values of each block of  $\mathbf{H}$* : The first step in the proposed low-complexity MMSE equalizer is the computation of the eigen values of  $\mathbf{H}$ . As discussed previously,  $\mathbf{H}$  has a block circulant structure with circulant blocks, with an eigen value decomposition of the form (12). The matrix  $\mathbf{\Lambda}$  in (12) can be written as

$$\begin{aligned} \mathbf{\Lambda} &= \sum_{i=0}^{M-1} \mathbf{\Omega}_M^i \otimes \mathbf{\Lambda}_i \\ &= \text{diag} \left\{ \sum_{i=0}^{M-1} \mathbf{\Lambda}_i, \sum_{i=0}^{M-1} e^{j2\pi i/M} \mathbf{\Lambda}_i, \dots, \sum_{i=0}^{M-1} e^{j2\pi(M-1)/M} \mathbf{\Lambda}_i \right\}, \end{aligned} \quad (17)$$

where  $\mathbf{\Lambda}_i$  denotes the  $N \times N$  diagonal matrix containing the eigen values of  $i$ th block in  $\mathbf{H}$ . The computation of eigen values of  $\mathbf{H}$  involves the following two steps: computing  $\mathbf{\Lambda}_i$ s by computing the eigen values of the circulant blocks of  $\mathbf{H}$  and computing  $\mathbf{\Lambda}$  using them as in (17). Since each block in  $\mathbf{H}$  has a circulant structure, the eigen values of each block are computed by computing the DFT of the first row of each block of  $\mathbf{H}$ . Therefore, computation of  $\mathbf{\Lambda}_1, \mathbf{\Lambda}_2, \dots, \mathbf{\Lambda}_M$  requires the computation of eigen values of  $M$  number of  $N \times N$  circulant matrices and hence has  $\mathcal{O}(MN \log N)$  complexity.

- 2) *Computation of the eigen values of  $\mathbf{H}$* : Next, using  $\mathbf{\Lambda}_i$ s, the eigen values of  $\mathbf{H}$  are computed using (17). A closer look at (17) reveals that the entries of  $\mathbf{\Lambda}$  can be computed with low complexity using IFFT. Let  $\mathbf{v}_1, \mathbf{v}_2, \dots, \mathbf{v}_M$  denote  $M$  column vectors of dimension  $N \times 1$  whose entries contain the diagonal elements of  $\mathbf{\Lambda}_1, \mathbf{\Lambda}_2, \dots, \mathbf{\Lambda}_M$ , respectively. Let  $\mathbf{V} = [\mathbf{v}_1^T \mathbf{v}_2^T \dots \mathbf{v}_M^T]^T$  denote the  $M \times N$  matrix whose rows are the vectors  $\mathbf{v}_1, \mathbf{v}_2, \dots, \mathbf{v}_M$ . Now, (17) can be computed as

$$\mathbf{\Lambda} = \text{diag}\{(\mathbf{F}_M^H \mathbf{V})^T\}. \quad (18)$$

The complexity of obtaining  $\mathbf{\Lambda}$  using (18) involves the computation of  $N$   $M$ -point IDFTs. Therefore, the complexity of this step is  $\mathcal{O}(MN \log M)$ .

- 3) *Computation of eigen values of  $\mathbf{G}_{\text{MMSE}}$* : Next, using the eigen values of  $\mathbf{H}$ , the eigen values of  $\mathbf{G}_{\text{MMSE}}$  are computed using (16). This step requires the computation of  $\Psi_1, \Psi_2, \dots, \Psi_{MN}$  using  $\lambda_1, \lambda_2, \dots, \lambda_{MN}$ , respectively. So the order of complexity for computing  $\mathbf{\Psi}$  is  $\mathcal{O}(MN)$ .
- 4) *Computation of  $\mathbf{G}_{\text{MMSE}} \mathbf{y}$* : The next step is to compute  $\mathbf{G}_{\text{MMSE}} \mathbf{y} = (\mathbf{F}_M \otimes \mathbf{F}_N)^H \mathbf{\Psi} (\mathbf{F}_M \otimes \mathbf{F}_N) \mathbf{y}$ . This equation can also be evaluated with low complexity using FFTs and IFFTs. Let  $\mathbf{Y}$  denote the  $N \times M$  matrix such that  $\text{vec}(\mathbf{Y}) = \mathbf{y}$ . Then,  $(\mathbf{F}_M \otimes \mathbf{F}_N) \mathbf{y}$  can be written as

$$\mathbf{z} = (\mathbf{F}_M \otimes \mathbf{F}_N) \mathbf{y} = \text{vec}(\mathbf{F}_N \mathbf{Y} \mathbf{F}_M^H). \quad (19)$$

Observe that  $\mathbf{z}$  can be obtained by computing  $N$ -point DFT along the columns of  $\mathbf{Y}$  and  $M$ -point IDFT along the rows of  $\mathbf{Y}$ . Thus, the complexity of computing  $\mathbf{z}$  using FFTs and IFFTs is  $\mathcal{O}(MN \log M + MN \log N) = \mathcal{O}(MN \log MN)$ . Next,  $\mathbf{\Psi} (\mathbf{F}_M \otimes \mathbf{F}_N) \mathbf{y}$  can be computed by computing  $\mathbf{\Psi} \mathbf{z}$ . Since  $\mathbf{\Psi}$  is a diagonal matrix, the computation of  $\mathbf{\Psi} \mathbf{z}$  has a complexity of  $\mathcal{O}(MN)$ . Now, let  $\mathbf{q} = \mathbf{\Psi} \mathbf{z}$  and  $\mathbf{Q}$  denote the  $N \times M$  matrix such that  $\text{vec}(\mathbf{Q}) = \mathbf{q}$ . With this,  $\mathbf{G}_{\text{MMSE}} \mathbf{y} = (\mathbf{F}_M \otimes \mathbf{F}_N)^H \mathbf{\Psi} (\mathbf{F}_M \otimes \mathbf{F}_N) \mathbf{y}$  can be computed as

$$\mathbf{G}_{\text{MMSE}} \mathbf{y} = \text{vec}(\mathbf{F}_N^H \mathbf{Q} \mathbf{F}_M). \quad (20)$$

Again, this step involves the computation of  $N$ -point IDFT along the columns of  $\mathbf{Q}$  and  $M$ -point DFT along the rows of  $\mathbf{Q}$ . Hence, this step has a complexity of  $\mathcal{O}(MN \log MN)$ . Therefore, the overall complexity of step 4 is  $\mathcal{O}(2MN \log MN + MN)$ .

## B. Low-complexity ZF equalizer

The transformation matrix for zero forcing detector is given by  $\mathbf{G}_{\text{ZF}} = (\mathbf{H}^H \mathbf{H})^{-1} \mathbf{H}^H$ . As discussed in the previous subsection, the  $\mathbf{H}$  is a block circulant matrix with circulant blocks and has an eigen value decomposition as in (12). Since  $\mathbf{G}_{\text{ZF}} = (\mathbf{H}^H \mathbf{H})^{-1} \mathbf{H}^H \in \mathcal{B}_{M,N}$ ,  $\mathbf{G}_{\text{ZF}}$  can be written as

$$\mathbf{G}_{\text{ZF}} = (\mathbf{F}_N \otimes \mathbf{F}_M)^H \mathbf{\Psi} (\mathbf{F}_N \otimes \mathbf{F}_M), \quad (21)$$

where  $\mathbf{\Psi} = (\mathbf{\Lambda}^* \mathbf{\Lambda})^{-1} \mathbf{\Lambda}^*$ . From the above equation, it is easy to see that the transformation matrix  $\mathbf{G}_{\text{ZF}}$  can be computed using FFTs, IFFTs, and diagonal matrix  $\mathbf{\Psi}$  containing the eigen values of  $\mathbf{G}_{\text{ZF}}$ . Also,  $\mathbf{\Psi} = (\mathbf{\Lambda}^* \mathbf{\Lambda})^{-1} \mathbf{\Lambda}^*$  can be obtained from  $\mathbf{\Lambda}$ , just by computing  $\lambda_i^* / |\lambda_i|^2 = 1/\lambda_i, i = 1, \dots, MN$ . The low-complexity ZF equalizer can be implemented as follows:

- 1) *Computation of eigen values of each block of  $\mathbf{H}$* : The eigen values of  $M$  circulant blocks of  $\mathbf{H}$  are computed using DFTs. The computational complexity of this step is  $\mathcal{O}(MN \log N)$ .
- 2) *Computation of eigen values of  $\mathbf{H}$* : The eigen values of  $\mathbf{H}$  ( $\mathbf{\Lambda}$ ) are computed using (17) as in the case of MMSE equalizer. This step can be implemented using IDFT as discussed in Sec. III-A and has a complexity of  $\mathcal{O}(MN \log M)$ .
- 3) *Computation of eigen values of  $\mathbf{G}_{\text{ZF}}$* : The eigen values of  $\mathbf{G}_{\text{ZF}}$  are computed using the eigen values of  $\mathbf{H}$  as

$$\mathbf{\Psi} = \text{diag}\{1/\lambda_1, 1/\lambda_2, \dots, 1/\lambda_{MN}\}. \quad (22)$$

The computational complexity of this step is  $\mathcal{O}(MN)$ .

4) *Computation of  $\mathbf{G}_{ZF}\mathbf{y}$* : The computation of  $\mathbf{G}_{ZF}\mathbf{y}$  is similar to the computation of  $\mathbf{G}_{MMSE}\mathbf{y}$  as in Sec. III-A. First,  $\mathbf{z} = (\mathbf{F}_M \otimes \mathbf{F}_N)\mathbf{y} = \text{vec}(\mathbf{F}_N \mathbf{Y} \mathbf{F}_M^H)$  is computed using  $N$ -point DFT along the columns of  $\mathbf{Y}$  and  $M$ -point IDFT along the rows of  $\mathbf{Y}$ . Next,  $\mathbf{q} = \mathbf{\Psi}\mathbf{z}$  is computed. Finally,  $\mathbf{G}_{ZF}\mathbf{y}$  is computed as  $\mathbf{G}_{ZF}\mathbf{y} = \text{vec}(\mathbf{F}_N^H \mathbf{Q} \mathbf{F}_M)$ , where  $\mathbf{q} = \text{vec}(\mathbf{Q})$ . Overall complexity of this step is  $\mathcal{O}(2MN \log MN + MN)$ .

The proposed algorithm is summarized as follows.

- 1: **Inputs:**  $\mathbf{y}$ ,  $\mathbf{H}$ .
- 2: **Step 1:** Compute eigen values of  $M$  circulant blocks of  $\mathbf{H}$  by computing DFTs of first row of each circulant block.
- 3: **Step 2:** Compute  $\mathbf{\Lambda}$  using (18).
- 4: **Step 3:** Compute  $\mathbf{\Psi}$  ( $\mathbf{\Psi} = (\mathbf{\Lambda}^* \mathbf{\Lambda} + \sigma^2 \mathbf{I})^{-1} \mathbf{\Lambda}^*$  in case of MMSE and  $\mathbf{\Psi} = (\mathbf{\Lambda}^* \mathbf{\Lambda})^{-1} \mathbf{\Lambda}^*$  in case of ZF).
- 5: **Step 4:** Compute  $\mathbf{G}_{MMSE}\mathbf{y}/\mathbf{G}_{ZF}\mathbf{y}$  by computing  $\mathbf{z} = \text{vec}(\mathbf{F}_N \mathbf{Y} \mathbf{F}_M^H)$ ,  $\mathbf{q} = \mathbf{\Psi}\mathbf{z}$ , and  $\text{vec}(\mathbf{F}_N^H \mathbf{Q} \mathbf{F}_M)$ .

The complexities associated with each step of the algorithm are presented in Table I. At this stage, we make the following remark on the proposed equalization approach.

TABLE I: Order of complexity.

Step #	Order of complexity
1: computation of eigen values of circulant blocks of $\mathbf{H}$	$\mathcal{O}(MN \log N)$
2: computation of $\mathbf{\Lambda}$	$\mathcal{O}(MN \log M)$
3: computation of $\mathbf{\Psi}$	$\mathcal{O}(MN)$
4: computation of $\mathbf{G}\mathbf{y}$	$\mathcal{O}(2MN \log MN + MN)$
Overall complexity (dominated by Step 4)	$\mathcal{O}(MN \log MN)$

*Remark:* It should be noted that the  $\mathbf{G}_{MMSE}$  and  $\mathbf{G}_{ZF}$  equalizers in the proposed approach perform equalization in the delay-Doppler domain, unlike the equalizers in [7],[8] which perform equalization in the TF domain. For the received signal to be accessed in the TF domain, the TF equalization approach requires the two-step OTFS implementation as in Fig. 1, viz., time domain to TF domain (using Wigner transform) and from TF domain to delay-Doppler domain (using SFFT). On the other hand, the proposed direct delay-Doppler equalization approach allows one-step OTFS implementation using Zak transform [2], which has significant complexity advantage compared to the two-step approach with TF equalization. Specifically, the implementation of OTFS with a single Zak transform has a complexity of  $MN \log N$  (as it involves the use of  $M$  FFTs of length  $N$ ), whereas the two-step OTFS implementation has a complexity of  $MN \log M + MN \log MN$ .

#### IV. RESULTS AND DISCUSSIONS

Figure 2a shows the BER performance comparison of OTFS with conventional ZF and MMSE equalizers and the proposed low-complexity ZF and MMSE equalizers. We consider a channel with  $P$  paths, with the  $i$ th path having a channel gain  $h_i$ , delay  $\tau_i$ , and Doppler  $\nu_i$ . The channel response in the delay-Doppler domain, denoted by  $h(\tau, \nu)$ , can be expressed as  $h(\tau, \nu) = \sum_{i=0}^{P-1} h_i \delta(\tau - \tau_i) \delta(\nu - \nu_i)$  [3]. The simulation set up considered in Fig. 2(a) uses the delay-Doppler value pairs for eight paths ( $P = 8$ ) as shown in the Table given below, where the  $i$ th path has delay  $\tau_i$  and Doppler  $\nu_i$ .

Path, $i$	1	2	3	4	5	6	7	8
$\tau_i$ ( $\mu\text{s}$ )	0	1.04	2.08	3.12	4.16	5.20	6.25	7.29
$\nu_i$ (Hz)	0	469	469	938	1406	1406	1875	1875

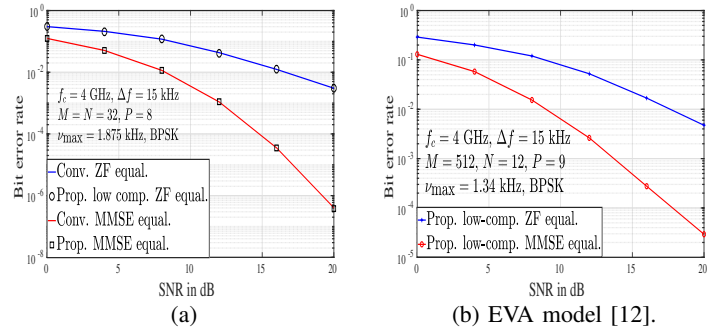


Fig. 2: BER performance of the proposed low-complexity ZF and MMSE equalizers.

The channel gains ( $h_i$ s) are assumed to be i.i.d and distributed as  $\mathcal{CN}(0, 1/P)$ . The signal-to-noise ratio (SNR) is defined as  $E[||\mathbf{H}\mathbf{x}||^2]/\sigma^2$ , where  $E[\cdot]$  denotes the expectation operator and  $\sigma^2$  is the noise variance. A delay Doppler grid with  $M = 32$  and  $N = 32$  is considered. A carrier frequency of 4 GHz, subcarrier spacing of 15 kHz, and BPSK modulation is considered. Firstly, from the figure, we observe that the performance of the MMSE equalizer is superior compared to that of the ZF equalizer. Further, the proposed low-complexity ZF and MMSE equalizers show exactly the same BER performance as that of the conventional ZF and MMSE equalizers, respectively. This demonstrates that, as expected, the proposed low-complexity algorithms provide the exact MMSE and ZF solutions and hence the same BER performance as that of the conventional MMSE and ZF equalizers. Figure 2b shows the BER performance of OTFS with the proposed low-complexity MMSE and ZF equalizers considering the channel parameters according to the extended vehicular A model (EVA) in 3GPP [12]. A channel with  $P = 9$  paths with a delay profile as per EVA model and Jakes Doppler spectrum is considered. The Doppler shifts  $\nu_i$ s corresponding to the  $i$ th path in different realizations are generated randomly using  $\nu_i = \nu_{\max} \cos \theta_i$ , where  $\nu_{\max}$  is the maximum Doppler shift which is taken to be 1.34 kHz, and  $\theta_i$ s are uniformly distributed over  $[-\pi, \pi]$ . A carrier frequency of 4 GHz, subcarrier spacing of 15 kHz, and frame size  $(M, N) = (512, 12)$  are considered. For the considered system with EVA channel model parameters recommended by 3GPP, the proposed low-complexity MMSE/ZF equalizers require 73731 real operations, whereas the conventional matrix inversion based equalizers require  $9.27 \times 10^{11}$  operations. Next, Fig. 3 shows the computational complexity of the conventional MMSE/ZF equalizers and the proposed low-complexity equalizers in terms of the number real operations involved as a function of  $M$ . For simulations,  $N = 32$  is considered and all other parameters are the same as those used in Fig. 2a. From Fig. 3, it can be observed that the complexity of the proposed MMSE equalizer is significantly less compared to that of conventional MMSE equalizer. For example, the number real operations required to compute MMSE solution for a system with  $M = 128$  and  $N = 32$  is  $2.75 \times 10^{11}$  in case of the conventional equalizer, whereas it is 49,155 in case of the proposed MMSE equalizer.

*Performance of OFDM based OTFS:* The OTFS implementation discussed so far used the TF modulation with ideal pulse satisfying biorthogonal and robustness property, for which

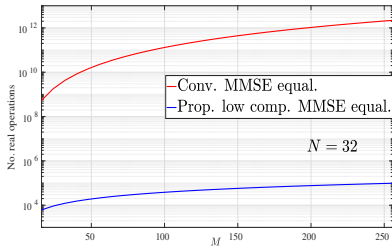


Fig. 3: Computational complexity of conventional and proposed low-complexity MMSE equalizers.

the input-output relation is of the form (5)<sup>†</sup>. However, for an OFDM based OTFS system [5] which uses rectangular pulse (non-ideal), the input-output relation in (5) does not hold and hence the effective channel matrix in the delay-Doppler domain will no longer have block circulant with circulant blocks structure. Hence, diagonalization of the effective channel matrix using  $\mathbf{F}_M \otimes \mathbf{F}_N$  may not yield a strictly diagonal matrix. As a result, the proposed low-complexity schemes may not yield exact MMSE/ZF solutions in OFDM based OTFS implementations. The effect of this observation is illustrated in Fig. 4a, which shows the performance of OFDM based OTFS. From Fig. 4a, we observe that the performance of the proposed low-complexity MMSE/ZF equalizers gets poor in OFDM based OTFS compared to that in OTFS with ideal pulse. This is because the proposed equalizers assume block circulant with circulant blocks structure for the effective channel matrix. However, as will be shown next, the proposed MMSE/ZF equalizer followed by a low-complexity non-linear equalizer achieves almost the same improved performance in OTFS with ideal pulse as well as OFDM based OTFS.

*Proposed MMSE equalizer followed by LAS equalizer:* We consider a local search based non-linear equalizer called likelihood ascent search (LAS) equalizer [10] following the proposed low-complexity linear equalizer. The LAS algorithm is a low-complexity algorithm that starts with an initial solution and searches for good solutions in the neighborhood until a local optimum is reached. The computational complexity of the LAS algorithm depends on the computation of the initial solution and the search operation. The complexity of obtaining an initial MMSE solution using conventional matrix inversion approach is  $\mathcal{O}(M^3N^3)$ , which is  $\mathcal{O}(M^2N^2)$  complexity per symbol. Further, it has been shown through simulations that the search operation in the LAS algorithm requires an average per-symbol complexity of  $\mathcal{O}(MN)$  [10]. The proposed low-complexity MMSE equalizer has a per-symbol complexity of  $\mathcal{O}(\log MN)$ . Therefore, the use of the proposed low-complexity MMSE equalizer to obtain the initial solution for the LAS algorithm significantly reduces the overall complexity. Figure 4b shows the BER performance of this MMSE-LAS equalizer for *i)* OTFS with ideal pulse and *ii)* OFDM based OTFS. From this figure, we observe that the performance of MMSE-LAS equalizer is significantly superior compared to that of the MMSE equalizer in both cases.

<sup>†</sup>Given the constraint imposed by the uncertainty principle, ideal pulses are non-realizable in practice. However, pulses whose support is highly concentrated in time and frequency minimize the cross-symbol interference, and hence closely approximate the ideal pulses. Design of such near-ideal pulses has been addressed in [9].

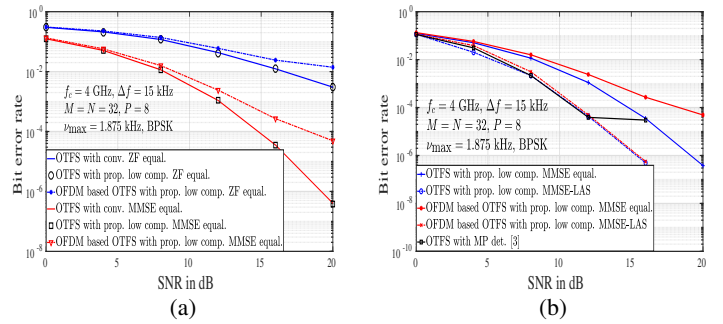


Fig. 4: Performance of proposed low-complexity ZF, MMSE equalizers and MMSE-LAS in OFDM based OTFS systems.

Importantly, though OFDM based OTFS with the proposed MMSE equalizer showed some degraded performance in Fig. 4a, we observe in Fig. 4b that the use of it with a LAS equalizer achieves almost the same improved performance compared to that of the use of it in OTFS with ideal pulse. This improved performance is achieved at a significantly low complexity. Figure 4b also shows the comparison of the BER performance of the proposed MMSE-LAS detector with the message passing (MP) based detection proposed in [3]. From this figure, we observe that MMSE-LAS and the MP detection have almost the same performance up to 12 dB SNR, after which the BER of MP detector floors, whereas the BER of MMSE-LAS detector continues to decrease. This is because the Gaussian approximation used in the computation of messages in MP detection involves sum of  $P - 1$  interference terms. Since  $P = 8$  in Fig. 4b, the approximation is less accurate because of the small number of terms involved in the approximation, and this leads to an error floor.

## REFERENCES

- [1] R. Hadani, S. Rakib, M. Tsatsanis, A. Monk, A. J. Goldsmith, A. F. Molisch, and R. Calderbank, "Orthogonal time frequency space modulation," in *Proc. IEEE WCNC'2017*, Mar. 2017, pp.1-7.
- [2] R. Hadani, S. Rakib, S. Kons, M. Tsatsanis, A. Monk, C. Ibars, J. Delfeld, Y. Hebron, A. J. Goldsmith, A. F. Molisch, and R. Calderbank, "Orthogonal time frequency space modulation," online: arXiv:1808.00519v1 [cs.IT] 1 Aug 2018.
- [3] P. Raviteja, K. T. Phan, Y. Hong, and E. Viterbo, "Interference cancellation and iterative detection for orthogonal time frequency space modulation," *IEEE Trans. Wireless Commun.*, vol. 17, no. 10, pp. 6501-6515, Aug. 2018.
- [4] K. R. Murali and A. Chockalingam, "On OTFS modulation for high-Doppler fading channels," in *Proc. ITA'2018*, Feb. 2018, pp. 1-10.
- [5] A. Farhang, A. R. Reyhani, L. E. Doyle, and B. Farhang-Boroujeny, "Low complexity modem structure for OFDM-based orthogonal time frequency space modulation," *IEEE Wireless Commun. Lett.*, vol. 7, no. 3, pp. 344-347, Jun. 2018.
- [6] A. Nimr, M. Chafii, M. Matthe, and G. Fettweis, "Extended GFDM framework: OTFS and GFDM comparison," in *Proc. IEEE GLOBECOM'2018*, Dec. 2018, pp. 1-6.
- [7] T. Zemen, M. Hofer, and D. Loeschbrand, "Low-complexity equalization for orthogonal time and frequency signaling (OTFS)," Online: arXiv:1710.09916v1 [cs.IT] 26 Oct 2017.
- [8] T. Zemen, M. Hofer, D. Loeschbrand, and C. Pacher, "Iterative detection for orthogonal precoding in doubly selective channels," in *Proc. IEEE PIMRC'2018*, Sep. 2018, pp. 1-7.
- [9] T. Strohmer and S. Beaver, "Optimal OFDM design for time-frequency dispersive channels," *IEEE Trans. Commun.*, vol. 51, no. 7, pp. 1111-1122, Jul. 2003.
- [10] A. Chockalingam and B. S. Rajan, *Large MIMO Systems*, Cambridge Univ. Press, Feb. 2014.
- [11] P. J. Davis, *Circulant Matrices*, American Mathematical Society, 2012.
- [12] *Evolved Universal Terrestrial Radio Access (E-UTRA); Base Station (BS) Radio Transmission and Reception*, 3GPP TS 36.104, Ver. 14.3.0, Rel. 14, Apr. 2017.